CHEMISTRY

# A chlorine-free protocol for processing germanium

Martin Glavinović,[1] Michael Krause,[2] Linju Yang,[3] John A. McLeod,[3] Lijia Liu,[3] Kim M. Baines,[2,3]* Tomislav Friščić,[1]* Jean-Philip Lumb[1]*



**Replacing molecular chlorine and hydrochloric acid with less energy- and risk-intensive reagents would markedly improve the environmental impact of metal manufacturing at a time when demand for metals is rapidly increasing. We describe a recyclable quinone/catechol redox platform that provides an innovative replacement for elemental chlorine and hydrochloric acid in the conversion of either germanium metal or germanium dioxide to a germanium tetrachloride substitute. Germanium is classified as a "critical" element based on its high dispersion in the environment, growing demand, and lack of suitable substitutes. Our approach replaces the oxidizing capacity of chlorine with molecular oxygen and replaces germanium tetrachloride with an air- and moisture-stable Ge(IV)-catecholate that is kinetically competent for conversion to high-purity germanes.**

## INTRODUCTION

The quality of modern life is increasingly dependent on the unique properties of metal-containing materials (*1*). This has prompted significant efforts to improve the efficiency of metal extraction and refinement, as well as metal recycling from postconsumer products (*2*). In mineral deposits and early stages of refinement, metals are typically present in the form of relatively inert oxides, whose processing is challenged by high lattice energies, high melting points, and low solubility (*3*). This requires their conversion into more labile derivatives for both purification and functionalization. Chief among these derivatives are metal chlorides, whose ubiquity in metal manufacturing belies an energy- and risk-intensive life cycle (Fig. 1A). Metal chlorides are prepared by either dehydration of the oxide with hydrochloric acid (HCl) or reduction of the oxide to the metal accompanied by reoxidation with molecular chlorine ($Cl_2$) (*3*). To appreciate the scale and impact of these processes, it is helpful to consider that the global synthesis of inorganic chemicals consumes ~$9 \times 10^6$ metric tons of $Cl_2$ per year, representing an energy demand exceeding $2 \times 10^{10}$ kWh, estimated by assuming the maximum efficiencies of the chlor-alkali process (*4*). The industrial synthesis of HCl is linked to $Cl_2$ by either reduction with hydrogen ($H_2$) or dehydrohalogenation of chlorinated organic compounds. Once produced, stringent regulations must be in place to transport and use $Cl_2$ and HCl, including corrosion-resistant facilities and precautions to rigorously maintain worker exposure below 1 and 5 parts per million (ppm) for $Cl_2$ and HCl, respectively. Many of these precautions must be maintained to manipulate downstream metal chlorides, which are generally moisture-sensitive and corrosive. The combination of these features creates clear motivations to replace $Cl_2$ and its associated products with more environmentally sensitive alternatives (*5*–*7*).

In their capacity as versatile intermediates for inorganic synthesis, metal chlorides provide invaluable flexibility, for which air- and moisture-tolerant replacements that do not use $Cl_2$ or HCl in their production are scarce (*8*). Metal chlorides are equally important in extraction and refinement processes. This requires a suitable replacement strategy to address issues of not only synthetic utility but also metal separation. In considering these challenges, we were drawn to metal complexes of catechols, which can be prepared from either a low-valent metal by two-electron oxidation with an *ortho*-quinone or substitution from a higher-valent metal with a catechol (Fig. 1B) (*9*). Although metal catecholates, and their related semiquinone redox tautomers, have been extensively studied as redox noninnocent ligands (*10*–*13*), their use as pseudohalides for inorganic synthesis has received considerably less attention (*14*, *15*). Ligand exchange of these complexes with a nucleophile could provide an organometallic complex retaining an oxidized metal center along with a displaced catechol (Fig. 1C). Assuming high efficiencies in the recovery of catechol, an attractive feature of this system could be its reoxidation to the *ortho*-quinone with air. This would close a redox cycle that ultimately links the oxidation of metals to the terminal reduction of molecular oxygen ($O_2$) in a manner that draws inspiration from Bäckvall's bioinspired electron transfer mediators for aerobic oxidations of organic substrates (*16*). This would replace the oxidizing capacity of $Cl_2$ with $O_2$, which could have a transformative effect on inorganic synthesis. $O_2$ is a readily available, naturally occurring oxidant, whose complete reduction to water ($H_2O$) provides a clean source of chemical energy that has been extensively investigated for improving the efficiency of organic synthesis (*17*, *18*). Current uses of $O_2$ in metal manufacturing are mostly limited to the synthesis of metal oxides, which suffer from the poor synthetic and processing utility discussed above. By segregating aerobic oxidation to the reoxidation of an organic cofactor, our system would draw from this naturally occurring and clean source of energy to drive inorganic synthesis while avoiding the formation of inert metal oxides.

To demonstrate the utility of this system, we report here a low-energy synthesis of organogermanes ($GeR_4$), including germane ($GeH_4$), from either germanium metal [Ge(0)] or germanium dioxide ($GeO_2$) (Fig. 1D). $GeH_4$ is widely used for the vapor deposition of germanium in electronic and optical device fabrication (*19*, *20*). Germanium is a nonrenewable resource that is classified by Licht *et al.* (*21*) as a "critical" element due to its low concentration in mineral ores, low producer diversity, lack of substitutes, and growing demand, which is estimated to increase by >2000% by 2050. This has led to new recovery efforts from postconsumer products, which accounted for ~30% of the 118 metric tons of germanium used industrially in 2011 (*21*). Although Ge(0) does not occur naturally, it is widely distributed in commercial products and is, thus, an important input into the industrial life cycle through postconsumer recycling, where it is first converted to germanium tetrachloride ($GeCl_4$) by oxidation with $Cl_2$ (*22*). Germanium is more

[1]Department of Chemistry, McGill University, 801 Sherbrooke Street West, Montreal, Quebec H3A 0B8, Canada. [2]Department of Chemistry, University of Western Ontario, 1151 Richmond Street, London, Ontario N6A 5B7, Canada. [3]Jiangsu Key Laboratory for Carbon-Based Functional Materials and Devices, Institute of Functional Nano and Soft Materials (FUNSOM) and Soochow University–Western University Center for Synchrotron Radiation Research, Soochow University, Suzhou, Jiangsu 215123 China.
*Corresponding author. Email: kbaines2@uwo.ca (K.B.); tomislav.friscic@mcgill.ca (T.F.); jean-philip.lumb@mcgill.ca (J.-P.L.)

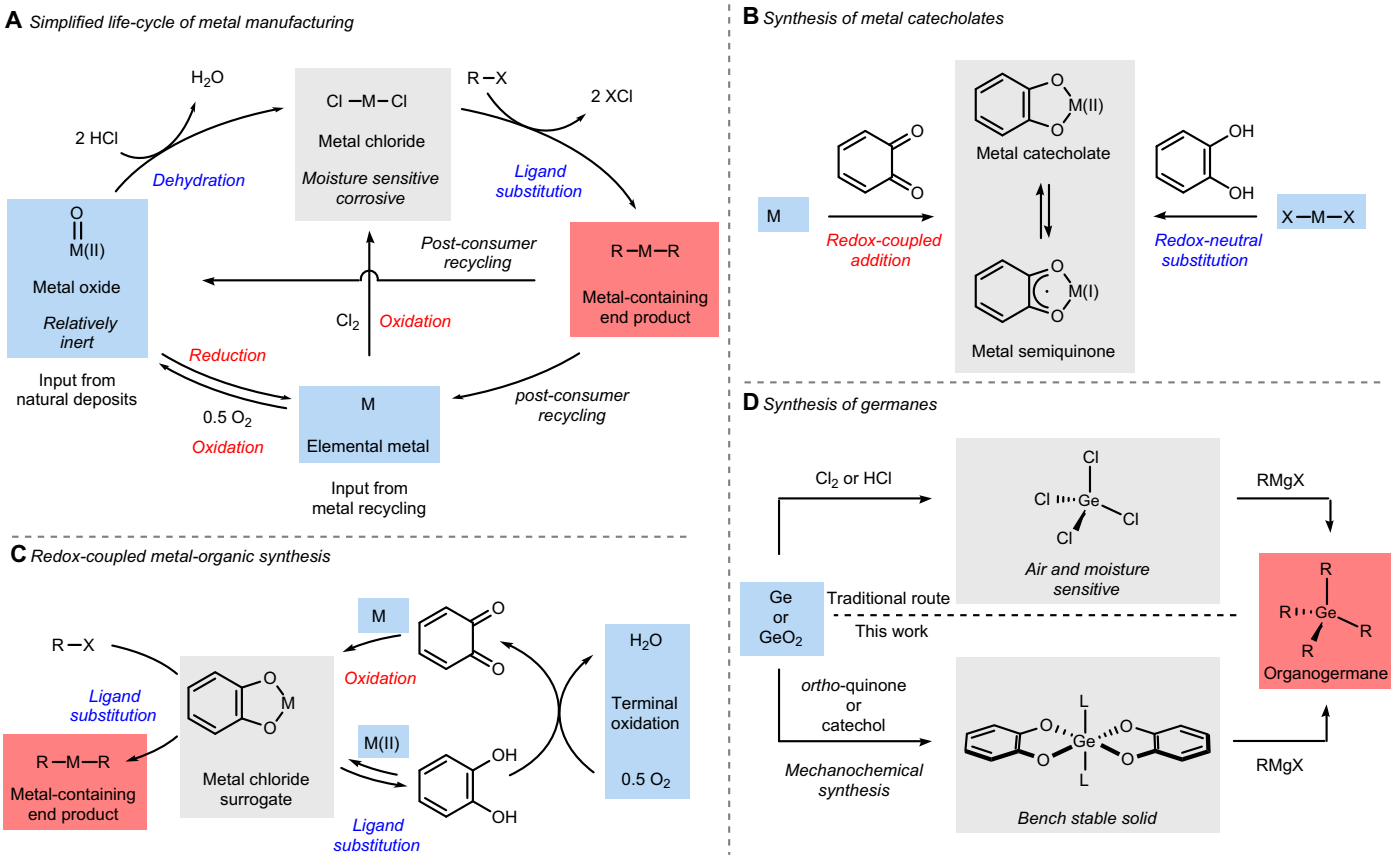


**Fig. 1. Strategies for the synthesis of metal-organic materials.** Steps in red represent a change in metal oxidation state, whereas those in blue are redox-neutral relative to the metal. (**A**) Simplified industrial life cycle of metal-containing materials. (**B**) Synthesis and redox isomerization of metal catecholates. (**C**) Aerobic oxidation of metals mediated by a quinone-catechol redox couple. (**D**) Synthesis of germanes from either germanium (Ge) or germanium dioxide ($GeO_2$).

commonly derived as a coproduct of zinc refinement, which requires a multistep extraction from zinc oxide (ZnO) that involves leaching distillation residues containing $GeO_2$ with HCl to produce $GeCl_4$ (*21*–*23*). As with many metal halides, $GeCl_4$ is a moisture-sensitive, corrosive liquid that hydrolyzes to HCl and $GeO_2$ in the presence of water. It is a poor reagent for substitution reactions (*14*), as evidenced by the low yields and low purity of $GeH_4$ streams that are produced by its reaction with metal hydrides (*20*) and the formation of incomplete substitution products and oligogermanes in its reaction with Grignard reagents (*24*). Nevertheless, $GeCl_4$ is a critical intermediate in the contemporary germanium life cycle, from which all downstream products are currently derived.

## RESULTS

Recognizing its central role, but energy- and risk-intensive use, we targeted a replacement of $GeCl_4$ that would exhibit bench-top stability and improved performance for the synthesis of germanes. Building upon early investigations by El-Hadad *et al.* (*25*) and our recent development of *ortho*-quinone **1** as a mild and selective metal oxidant (*9*) that is readily synthesized from the bulk chemicals phenol and isobutylene (*26*), we evaluated the mechanochemical (*27*) oxidation of Ge powder (1 equiv) by ball milling with quinone **1** (2 equiv) in the presence of pyridine (Py) (2 equiv) as an auxiliary ligand (Fig. 2A). The use of liquid-assisted grinding (LAG) conditions was paramount (*28*), because efforts to grind the reactants in neat form returned unreacted starting materials, as determined by powder x-ray diffraction (PXRD) (fig. S2). By contrast, the addition of 60 μl of a 1:1 mixture of toluene (PhMe) and water ($H_2O$) for a total reactant mass of 200 mg provided complex **3** in 88% isolated yield following milling at 30 Hz for 3 hours at room temperature and recrystallization from toluene. This efficiency was maintained on gram scale to provide complex **3** in 83% isolated yield. Complex **3** is a bench-top stable, beige solid, whose structure was unambiguously identified by nuclear magnetic resonance (NMR) spectroscopy, single-crystal x-ray crystallography, and x-ray absorption spectroscopy (XAS) (Fig. 2, B and C, and the Supplementary Materials). The octahedral complex has the two pyridine ligands in trans-disposition with a Ge–N(1) bond length of 2.098(1) Å, which is comparable to the Ge–N distances in a series of pyridyl Ge(IV) halide complexes (2.01 to 2.11 Å) (*29*–*32*). Not surprisingly, the pyridine nitrogen–germanium bond distances are elongated compared to standard Ge–N acyclic bond distances (1.85 to 1.86 Å) (*33*). The catecholato ligands are arranged in a plane about the germanium [O–Ge–O bond angles of 89.41(5)° and 90.59(5)°]. The Ge–O bond distances of 1.847(1) and 1.849(1) Å fall clearly within the range reported for related bis(catecholato)Ge(IV) complexes with alcohol- or ether-based donor ligands (*33*–*35*). The C–O bond distances of 1.366(2) and 1.365(2) Å are typical for catecholate ligands (*10*), suggesting a two-electron reduction of each *ortho*-quinone unit and a net oxidation of Ge(0) to Ge(IV). This assignment was further established using XAS: Fig. 2C compares the Ge K-edge XAS of complex **3** with two Ge(IV) reference materials, $GeO_2$ and $Ge(HPO_4)_2$ (see also fig. S14). Ge K-edge XAS

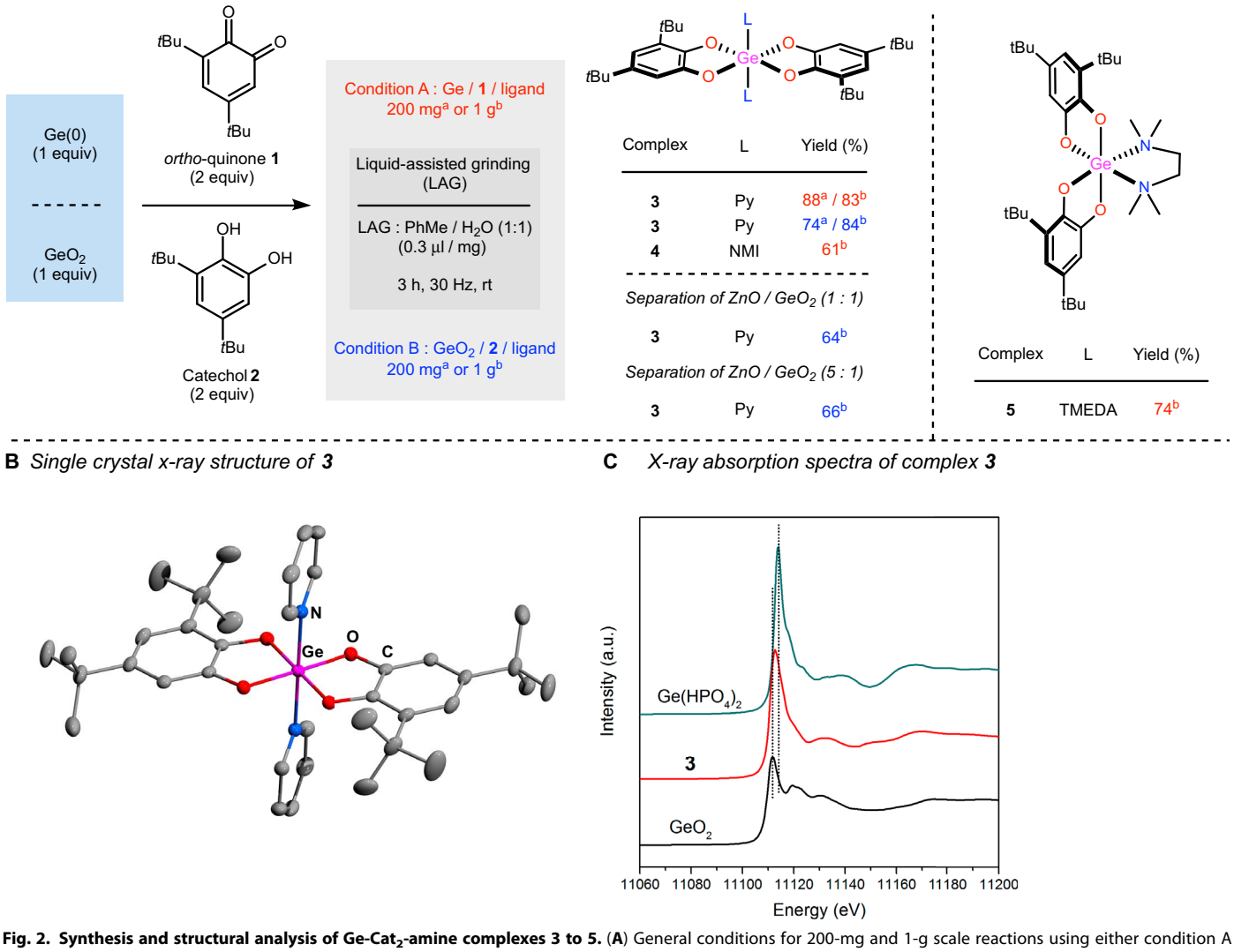


**Fig. 2. Synthesis and structural analysis of Ge-Cat$_2$-amine complexes 3 to 5.** (**A**) General conditions for 200-mg and 1-g scale reactions using either condition A [Ge(0) (1 equiv) and **1** (2 equiv)] or condition B [$GeO_2$ (1 equiv) and **2** (2 equiv)] along with ligand (only 1 equiv of TMEDA was used) (2 equiv), liquid (60 or 300 µl of a 1:1 volumetric mixture of PhMe/$H_2O$), and milling frequency (30 Hz) at room temperature for 3 hours. Optimization of the reaction conditions is described in the Supplementary Materials (figs. S1 to S9). Reported yields are for isolated complexes following recrystallization. (**B**) Single-crystal x-ray structure for complex **3** (toluene), with toluene and hydrogens removed for clarity (fig. S43 and table S6). (**C**) Ge K-edge X-ray absorption spectrum of **3** using $Ge(HPO_4)_2$ and $GeO_2$ as reference materials.

monitors the change of absorption coefficient when a Ge 1s electron is excited to previously unoccupied states of *p* character. The energy position of the absorption threshold is sensitive to the electron density (that is, oxidation state) at the element of interest. In general, the energy onset of compounds with higher oxidation states appears at higher excitation energy. The spectral profile after the absorption threshold is the fingerprint region, which is strongly affected by the local coordination of the element probed. $GeO_2$ and $Ge(HPO_4)_2$ both have a nominal oxidation state of (IV), so the absorption thresholds are at similar locations. Ge with lower oxidation states is expected to have an absorption onset at much lower energy (*36*). The local environment about the Ge core in complex **3** and the two reference compounds are almost identical, as indicated by the similarities of their spectral profiles. The absorption peak maximum of complex **3** falls between that of $GeO_2$ and $Ge(HPO_4)_2$, confirming that the Ge center has an oxidation state of (IV).

The mechanochemical protocol for the synthesis of **3** provides flexibility in the choice of the amine ligand, which in turn provides a means of controlling the relative stereochemistry of the catecholate complex (Fig. 2A). For example, replacing Py with *N*-methyl-imidazole (NMI) affords an isostructural octahedral complex **4** with trans-disposed nitrogen ligands, whereas a cis relationship between the nitrogen atoms can be enforced by using a chelating diamine, so that tetramethylethylenediamine (TMEDA) provides octahedral complex **5** under otherwise identical conditions. As with complex **3**, the structures of complexes **4** and **5** were unambiguously determined by single-crystal x-ray diffraction and NMR spectroscopy, and their metrical parameters fall within the expected ranges (figs. S15 to S20, S44, and S45).

Our optimized LAG conditions can be extended to the dehydration of $GeO_2$ by simply replacing quinone **1** with catechol **2** (2 equiv) under otherwise identical conditions (see Fig. 2A and the Supplementary

Materials) (*14*, *35*). This provides complex **3** in 84% isolated yield on a gram scale. Activation of metal oxides at room temperature in a chloride-free process that generates $H_2O$ as the sole stoichiometric by-product is noteworthy (*37*) and allows us to approach the challenge of oxide separation under mild conditions. From natural deposits, germanium is separated from ZnO by leaching with HCl to provide mixtures of $GeCl_4$ and $ZnCl_2$ that are separated by distillation (boiling point of $GeCl_4$, 86.5°C; boiling point of $ZnCl_2$, 732°C) (*21*–*23*). By using our mechanochemical approach, we can selectively functionalize $GeO_2$ in both 1:1 and 1:5 mixtures with ZnO (by weight) by simply milling with catechol **2** under our standard conditions. This selectively activates $GeO_2$ as the bis(catecholate) complex, which is readily separated from ZnO by washing with methylene chloride (*37*). Complex **3** is then isolated in yields of 64 and 66%, respectively, following recrystallization from cyclohexane. This provides a proof-of-principle demonstration of a low-energy and chloride-free approach for the separation of germanium from zinc.

The relative stability of catecholate complexes **3** to **5** does not compromise their participation in substitution reactions with carbon nucleophiles, which provides the corresponding tetraorganogermanes in high yield and purity (Fig. 3). Under our optimized conditions, a solution of an alkyl or aryl Grignard reagent (20 equiv) in tetrahydrofuran (THF) is added to a suspension of **3** in THF. The resulting heterogeneous mixture is then warmed to 65°C for 24 hours before aqueous workup and chromatographic separation to provide the organogermanes with isolated yields generally above 80%. Substitution with BnMgCl presents an exception (entry 8), where we attribute the decreased yield of 60% to competitive formation of bibenzyl. Substitution with allylMgCl proceeds in near-quantitative yield (entry 9) and provides a favorable point of comparison to the related substitution using $GeCl_4$, which proceeds in only 45% yield (*38*). In each of these cases, the unusually high selectivity and isolated yield of the organogermanes are accompanied by good to excellent recoveries of catechol **2.** This allows us to indirectly link the four-electron oxidation of Ge(0) to the reduction of $O_2$ by using well-established methodologies for the catalytic aerobic oxidation of catechol **2** to quinone **1** (*39*).

We attribute the unusually high selectivity for the substitution reaction of complex **3** to a unique mechanism, in which steric strain is relieved as substitution progresses (Fig. 4A) (*15*). This is distinct from substitution reactions of $GeCl_4$, where exchange of a chloride ligand with a carbon nucleophile creates a more sterically encumbered complex,

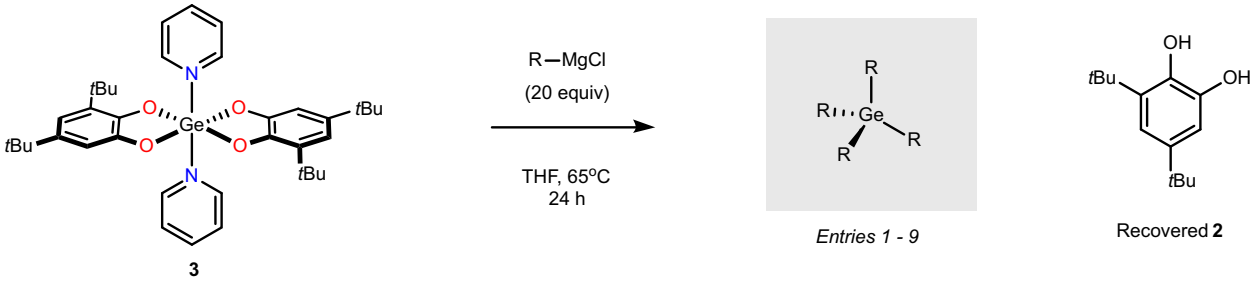


| Entry | R | Yield (%) | Recovered **2** (%) |
|---|---|---|---|
| 1 | $-(CH_2)_3CH_3$ | 91 | 92 |
| 2[a] | $-(CH_2)_3CH_3$ | 89 | 89 |
| 3[b] | $-(CH_2)_3CH_3$ | 96 | 99 |
| 4 | $-(CH_2)_5CH_3$ | 97 | 67 |
| 5[c] | $-CH_3$ | 100 | --- |

| Entry | R | Yield (%) | Recovered **2** (%) |
|---|---|---|---|
| 6 | H | 83 | 83 |
| 7 | Me | 85 | 91 |

| Entry | Yield (%) | Recovered **2** (%) |
|---|---|---|
| 8[d] | 60 | 74 |

| Entry | Yield (%) | Recovered **2** (%) |
|---|---|---|
| 9 | 97 | 80 |

**Fig. 3. Scope of substitution reaction.** General conditions: **3** (250 mg), RMgCl (20 equiv), THF (10 ml), 65°C for 24 hours. [a]Complex **4** used in place of complex **3.** [b]Complex **5** used in place of complex **3.** [c]Using MeMgBr in $Bu_2O$; $^1$H NMR yield using toluene as an internal standard. [d]Isolated as a 10:1 mixture with bibenzyl.

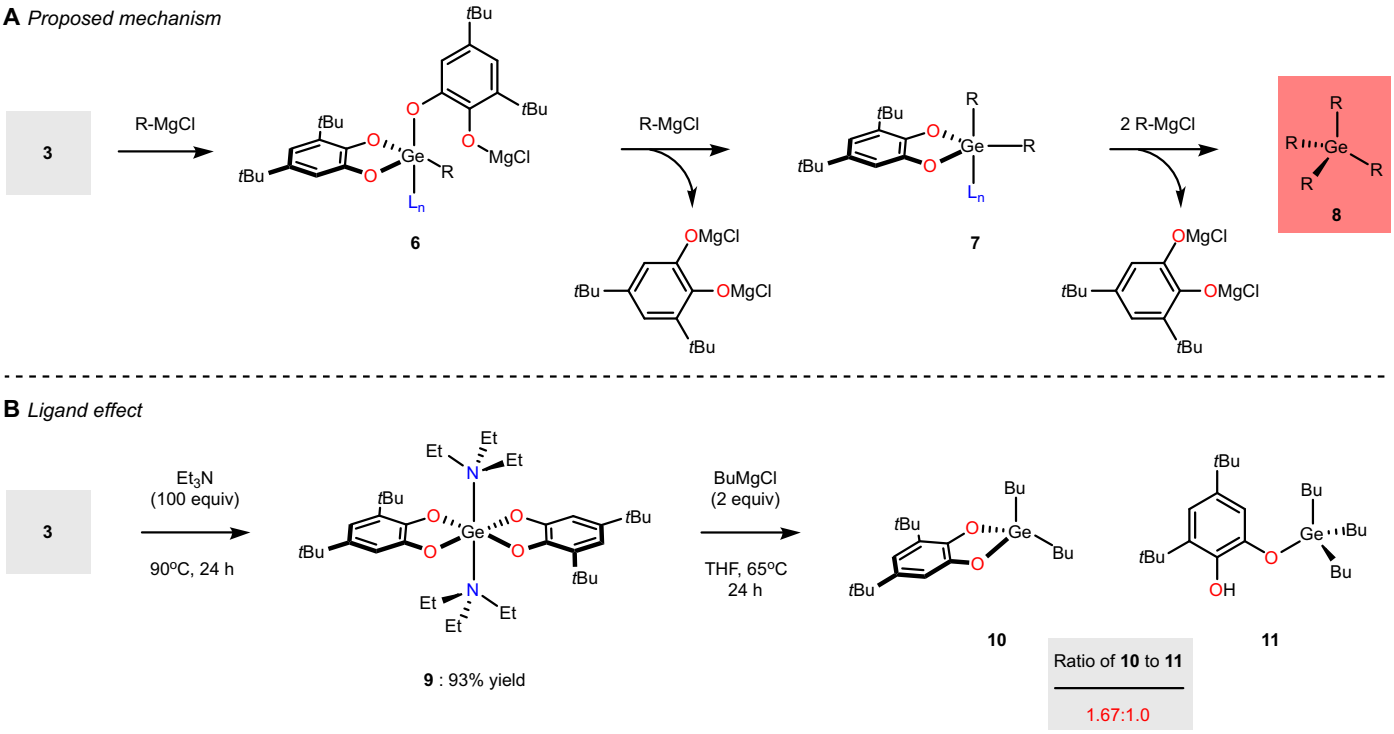


**Fig. 4. Proposed mechanism and ligand effects.** (**A**) Substitution occurs by an increasingly facile replacement of the catecholate ligand with the Grignard reagent. (**B**) Effects of a more Lewis basic and sterically encumbered amine ligand.

so that substitution becomes increasingly difficult as the reaction progresses. In contrast, partially replacing the catecholate ligands of **3** should create a more accessible germanium center, so that substitution of **6** with a second equivalent of the Grignard reagent to provide **7** is faster than the first. Subsequent substitution of **7** with two additional equivalents of the Grignard reagent to provide organogermane **8** should then become increasingly facile, because the sterically encumbered catecholate ligands are progressively displaced. Recognizing that the course of the substitution reaction should be influenced by the amine ligand, we investigated the reactivity of complex **9**, in which the pyridine ligands in complex **3** are replaced by more sterically encumbered and Lewis basic triethylamine ($Et_3N$) ligands (Fig. 4B). In this case, reaction of complex **9** with two equivalents of BuMgCl returns a 1.67:1 mixture of dibutyl-germane-$\eta^2$-catecholate **10** and tributylgermyl-$\eta^1$-catecholate **11** in a combined yield of 84%. The regiochemistry depicted for catecholate **11** is supported by two-dimensional NMR experiments (see section S6J for additional discussion) and supports our steric model, in which the more encumbered of the two oxygen ligands is released first from the Ge center. These results demonstrate an important influence of the amine ligand over chemoselectivity, which should open new opportunities for the synthesis of more highly functionalized germanes.

Recognizing the unique performance of complex **3** in the complete and selective fourfold substitution reaction with Grignard reagents, we evaluated its performance as a precursor to $GeH_4$ using lithium aluminum hydride ($LiAlH_4$) as a hydride donor (Fig. 5). $GeH_4$ is a volatile, highly flammable, and toxic gas at room temperature, whose considerable risks are offset by its high value as a reagent for vapor deposition (*19*). Because of stringent requirements of purity, the preparation and purification of $GeH_4$ have been extensively studied (*20*, *40*). Existing methodologies starting from Ge include electrochemical oxidation, plasma-based bombardment with high-energy protons, or sintering with alkaline earth metals to provide germanides (for example, $Mg_2Ge$) followed by protonation. More commonly practiced are chemical reductions of $GeCl_4$, $GeO_2$, or $Na_2GeO_3$ with metal hydrides in either organic solvents or aqueous solutions below pH 7. Drawbacks to these methodologies include any one or more of the following: use of highly purified Ge, $GeCl_4$, or $GeO_2$; high-energy demands; and the coproduction of unwanted by-products, including digermane ($Ge_2H_6$) (*20*, *40*). To address the challenge of preparing a high-quality $GeH_4$ stream, we evaluated the substitution of complex **3** with $LiAlH_4$ at room temperature using dibutyl ether as solvent and argon (Ar) as an inert carrier gas (Fig. 5A). Substitution reactions were performed in a modified J. Young tube reactor directly connected to a mass spectrometer with a detection limit of ~20 fg. Upon agitation of a heterogeneous mixture of complex **3** and $LiAlH_4$, moderate gas evolution was observed for ~20 min. The resulting headspace was then directly sampled by electron impact mass spectrometry (EI-MS) (see Fig. 5B and the Supplementary Materials) to reveal only the formation of $GeH_4$ as a gaseous mixture with Ar, with no other volatile compounds being detected over the course of the experiment. Analysis of the resulting liquid phase by $^1H$ NMR spectroscopy was equally clean, showing only unreacted $LiAlH_4$ and no sign of oligomeric germanes. Comparably pure germane streams from $GeO_2$ or $GeCl_4$ require postsynthesis purification, suggesting that complex **3** may provide a number of competitive advantages.

## DISCUSSION

The quinone/catechol redox platform described here provides a valuable strategy for addressing issues of sustainability in metal-organic synthesis. Although calls to reduce, and in some cases ban, the use of $Cl_2$

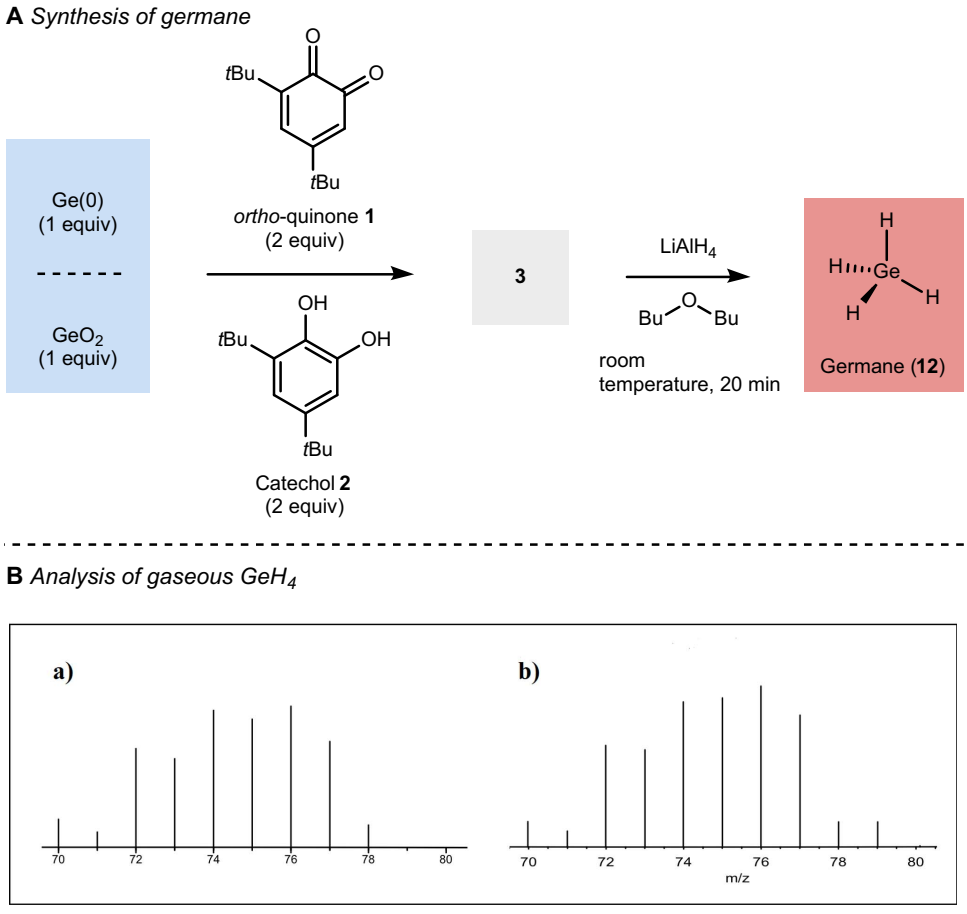


**Fig. 5. Synthesis of germane from 3.** (**A**) Reaction conditions: $LiAlH_4$ (12 mg), **3** (44 mg), room temperature, $Bu_2O$ (1 ml). (**B**) Isotopic distribution of $GeH_4$ signal (EI-MS): a, calculated; b, experimental.

and HCl have been made (*5*, *6*), few technologies to enable these reductions are available. The current system provides a unique mechanism to replace the oxidative capacity of $Cl_2$ with $O_2$ while preserving the functional utility of metal chlorides in both separations and downstream synthetic transformations. Given the ubiquity of metal chlorides in metal-organic manufacturing and the precedent for oxidizing a range of transition metals with *ortho*-quinones, we anticipate a number of opportunities beyond germanium for applying this system.

## METHODS

### Mechanochemical oxidation of germanium with *ortho*-quinone

Stainless steel milling jars (10 ml for 200-mg scale, 25 ml for 1-g scale) were equipped with two 6-mm-diameter stainless steel balls and charged with Ge powder (1 equiv), 3,5-di-*tert*-butyl-*ortho*-benzoquinone (**1**) (2 equiv), and 2 equiv of a monodentate amine ligand (Py or NMI) or 1 equiv of a diamine ligand (TMEDA). A 1:1 mixture of PhMe/$H_2O$ (v/v) (60 μl for 200-mg scale or 300 μl for 1-g scale) was then added to this mixture. The jars were then sealed, and the mixtures were milled with a Retsch MM 400 mill for 180 min at a frequency of 30 Hz. The resulting crude reaction mixture was then dissolved with PhMe, filtered, and recrystallized from cyclohexane to afford the pure Ge(IV) catecholates.

### Mechanochemical activation of germanium oxide with catechol

Stainless steel milling jars (10 ml for 200-mg scale, 25 ml for 1-g scale) were equipped with two 6-mm-diameter stainless steel balls and charged with $GeO_2$ (1 equiv), 3,5-di-*tert*-butyl-catechol (**2**) (2 equiv), and 2 equiv of a monodentate amine ligand (**Py** or **NMI**) or 1 equiv of a diamine ligand (**TMEDA**). A 1:1 mixture of PhMe/$H_2O$ (v/v) (60 μl for 200-mg scale or 300 μl for 1-g scale) was then added to this mixture. The jars were then sealed, and the mixtures were milled with a Retsch MM 400 mill for 180 min at a frequency of 30 Hz. The resulting crude reaction mixture was then dissolved with PhMe, filtered, and recrystallized to afford the pure Ge(IV) catecholates.

### Synthesis of tetraorganogermanes from Ge(IV) bis(catecholate) complexes

A 100-ml round-bottom flask, equipped with a Teflon-coated magnetic stirring bar and a reflux condenser, was charged with the Ge(IV) catecholate (0.372 mmol; 1 equiv) and a solvent corresponding to the solvent of the Grignard reagent (6.25 ml). The Grignard reagent (8 mmol; 20 equiv) was added to this suspension. The resulting mixture was then warmed to 65°C and kept at this temperature for 24 hours. After cooling to room temperature, hexanes (15 ml) were added to the crude reaction mixture followed by $H_2O$ (5 ml), and the reaction mixture

was vigorously stirred for 5 min. The layers were then separated, and the organic layer was washed with $H_2O$ (5 ml), separated, and concentrated using a rotary evaporator. Purification of the resulting crude reaction mixture was then carried out using preparative thin layer chromatography to provide the tetraorganogermane in pure form.

## SUPPLEMENTARY MATERIALS

Supplementary material for this article is available at http://advances.sciencemag.org/cgi/content/full/3/5/e1700149/DC1

Supplementary Materials and Methods
section S1. General experimental
section S2. General procedures
section S3. Optimization of the mechanochemical synthesis of complex **3**
section S4. Synthesis and characterization of complexes
section S5. Synthesis of organogermanes
section S6. Characterization data
section S7. Single-crystal x-ray diffraction
fig. S1. PXRD patterns; initial experiments.
fig. S2. PXRD data for the optimized synthesis of complex **3**, exploring the liquid additive in LAG.
fig. S3. PXRD data for the optimized synthesis of complex **3**, exploring the volume of liquid additive in LAG.
fig. S4. PXRD data for the optimized synthesis of complex **3**, exploring Py equivalents.
fig. S5. PXRD data for the optimized synthesis of complex **3**, exploring different milling reaction times.
fig. S6. PXRD data for the optimized synthesis of complex **3**, exploring milling frequency.
fig. S7. PXRD data for the optimized 1-g scale synthesis of complex **3**, exploring milling frequency.
fig. S8. PXRD data for the optimized 1-g scale synthesis of complexes **4** and **5**.
fig. S9. PXRD data for the optimized synthesis of complex **3** from $GeO_2$.
fig. S10. PXRD data for the optimized synthesis of complex **3** from $GeO_2$/ZnO mixtures.
fig. S11. Reaction apparatus for generating $GeH_4$.
fig. S12. $^1$H NMR (500 MHz, $CDCl_3$) spectrum of complex **3**.
fig. S13. Thermogravimetric analysis (TGA) of complex **3**.
fig. S14. First derivatives of the Ge K-edge XAS of complex **3** compared to $Ge(HPO_4)_2$ and $GeO_2$ as reference materials.
fig. S15. $^1$H NMR (500 MHz, $CDCl_3$) spectrum of complex **4**.
fig. S16. $^{13}$C NMR (125 MHz, $CDCl_3$) spectrum of complex **4**.
fig. S17. TGA of complex **4**.
fig. S18. $^1$H NMR (500 MHz, $CDCl_3$) spectrum of complex **5**.
fig. S19. $^{13}$C NMR (125 MHz, $CDCl_3$) spectrum of complex **5**.
fig. S20. TGA of complex **5**.
fig. S21. $^1$H NMR (400 MHz, $CDCl_3$) spectrum of $GeBu_4$ (inset, expansion from 1.45 to 0.60 ppm).
fig. S22. $^{13}$C NMR (100 MHz, $CDCl_3$) spectrum of $GeBu_4$ (inset, expansion from 28 to 12 ppm).
fig. S23. $^1$H NMR (400 MHz, $CDCl_3$) spectrum of $GePh_4$ (inset, expansion from 7.65 to 7.35 ppm).
fig. S24. $^{13}$C NMR (100 MHz, $CDCl_3$) spectrum of $GePh_4$ (inset, expansion from 137 to 127 ppm).
fig. S25. $^1$H NMR (400 MHz, $CDCl_3$) spectrum of $GeBn_4$ (inset, expansion from 7.30 to 6.80 ppm).
fig. S26. $^{13}$C NMR (100 MHz, $CDCl_3$) spectrum of $GeBn_4$ (inset, expansion from 128.5 to 128.0 ppm).
fig. S27. $^1$H NMR (600 MHz, $CDCl_3$) spectrum of $Ge((CH_2)_5CH_3)_4$ (inset, expansion from 1.40 to 0.65 ppm).
fig. S28. $^{13}$C NMR (150 MHz, $CDCl_3$) spectrum of $Ge((CH_2)_5CH_3)_4$.
fig. S29. $^1$H NMR (400 MHz, $CDCl_3$) spectrum of $Ge(CH_2–CH=CH_2)_4$.
fig. S30. $^1$H NMR (400 MHz, $CDCl_3$) spectrum of $Ge(CH_2–CH=CH_2)_4$ from 1.86 to 1.70 ppm.
fig. S31. $^1$H NMR (400 MHz, $CDCl_3$) spectrum of $Ge(CH_2–CH=CH_2)_4$ from 5.90 to 4.80 ppm.
fig. S32. $^{13}$C NMR (100 MHz, $CDCl_3$) spectrum of $Ge(CH_2–CH=CH_2)_4$.
fig. S33. $^1$H NMR (600 MHz, $CDCl_3$) spectrum of Ge(p-Tol)$_4$ (inset, expansion from 7.50 to 7.15 ppm).
fig. S34. $^{13}$C NMR (150 MHz, $CDCl_3$) spectrum of Ge(p-Tol)$_4$.
fig. S35. $^1$H NMR (600 MHz, $CDCl_3$) spectrum of complex **11**.
fig. S36. $^1$H NMR (600 MHz, $CDCl_3$) spectrum of complex **11** from 1.55 to 0.85 ppm.
fig. S37. $^{13}$C NMR (150 MHz, $CDCl_3$) spectrum of complex **11**.
fig. S38. $^{13}$C NMR (150 MHz, $CDCl_3$) spectrum of complex **11** from 112.50 to 111.50 ppm.
fig. S39. $^{13}$C NMR (150 MHz, $CDCl_3$) spectrum of complex **11** from 40 to 10 ppm.
fig. S40. Two possible isomers for complex **11**.
fig. S41. Expansion of the $^{13}$C-$^1$H HSQC spectrum of complex **11**.
fig. S42. Expansion of the $^{13}$C-$^1$H HMBC spectrum of complex **11**.
fig. S43. Thermal ellipsoid plot of Ge(3,5-dtbc)$_2$(Py)$_2$·2PhMe (**3**).
fig. S44. Thermal ellipsoid plot of Ge(3,5-dtbc)$_2$(NMI)$_2$·DCM (**4**).
fig. S45. Thermal ellipsoid plot of Ge(3,5-dtbc)$_2$(TMEDA)·2DCM (**5**).
table S1. Optimization of LAG additive composition.
table S2. Optimization of LAG additive volume.
table S3. Optimization of Py equivalents.
table S4. Optimization of milling time.
table S5. Optimization of milling frequency.
table S6. Crystal data and structure refinement parameters for complexes **3** and **5**.
References (*41*–*42*)

## REFERENCES AND NOTES


1. T. E. Graedel, E. M. Harper, N. T. Nassar, B. K. Reck, On the materials basis of modern society. *Proc. Natl. Acad. Sci. U.S.A.* **112**, 6295–6300 (2015).
2. E. D. Doidge, I. Carson, P. A. Tasker, R. J. Ellis, C. A. Morrison, J. B. Love, A simple primary amide for the selective recovery of gold from secondary resources. *Angew. Chem., Int. Ed.* **55**, 12436–12439 (2016).
3. J. J. Moore, in *Chemical Metallurgy* (Butterworth-Heinemann, ed. 2, 1990), pp. 243–309.
4. P. Schmittinger, T. Florkiewicz, L. Calvert Curlin, B. Lüke, R. Scannell, T. Navin, E. Zelfel, R. Bartsch, Chlorine, in *Ullmann's Encyclopedia of Industrial Chemistry* (Wiley-VCH Verlag GmbH & Co. KGaA, 2000), pp. 532–622.
5. R. Ayers, The life-cycle of chlorine, Part I: Chlorine production and the chlorine-mercury connection. *J. Ind. Ecol.* **1**, 81–94 (1997).
6. C. C. Cummins, Phosphorus: From the stars to land & sea. *Daedalus* **143**, 9–20 (2014).
7. A. Czaja, E. Leung, N. Trukhan, U. Müller, Industrial MOF synthesis, in *Metal-Organic Frameworks* (Wiley-VCH Verlag GmbH & Co. KGaA, 2011), pp. 337–352.
8. M. N. Temnikov, A. S. Zhiltsov, V. M. Kotov, I. V. Krylova, M. P. Egorov, A. M. Muzafarov, Comparison of effectiveness of various approaches to direct synthesis of alkoxysilanes. *Silicon* **7**, 69–78 (2015).
9. M. Glavinović, F. Qi, A. D. Katsenis, T. Friščić, J.-P. Lumb, Redox-promoted associative assembly of metal–organic materials. *Chem. Sci.* **7**, 707–712 (2016).
10. C. G. Pierpont, R. M. Buchanan, Transition metal complexes of *o*-benzoquinone, *o*-semiquinone, and catecholate ligands. *Coord. Chem. Rev.* **38**, 45–87 (1981).
11. L. Sun, M. G. Campbell, M. Dincă, Electrically conductive porous metal-organic frameworks. *Angew. Chem., Int. Ed.* **55**, 3566–3579 (2016).
12. Z. Huang, J.-P. Lumb, A catalyst-controlled aerobic coupling of *ortho*-quinones and phenols applied to the synthesis of aryl ethers. *Angew. Chem., Int. Ed.* **55**, 11543–11547 (2016).
13. L. E. Darago, M. L. Aubrey, C. J. Yu, M. I. Gonzalez, J. R. Long, Electronic conductivity, ferrimagnetic ordering, and reductive insertion mediated by organic mixed-valence in a ferric semiquinoid metal–organic framework. *J. Am. Chem. Soc.* **137**, 15703–15711 (2015).
14. G. Cerveau, C. Chuit, R. J. P. Corriu, C. Reye, Reactivity of dianionic hexacoordinate germanium complexes toward organometallic reagents. A new route to organogermanes. *Organometallics* **10**, 1510–1515 (1991).
15. C. Chuit, R. J. P. Corriu, C. Reye, J. C. Young, Reactivity of penta- and hexacoordinate silicon compounds and their role as reaction intermediates. *Chem. Rev.* **93**, 1371–1448 (1993).
16. J. Piera, J.-E. Bäckvall, Catalytic oxidation of organic substrates by molecular oxygen and hydrogen peroxide by multistep electron transfer—A biomimetic approach. *Angew. Chem. Int. Ed.* **47**, 3506–3523 (2008).
17. T. Punniyamurthy, S. Velusamy, J. Iqbal, Recent advances in transition metal catalyzed oxidation of organic substrates with molecular oxygen. *Chem. Rev.* **105**, 2329–2363 (2005).
18. A. E. Wendlandt, A. M. Suess, S. S. Stahl, Copper-catalyzed aerobic oxidative C-H functionalizations: Trends and mechanistic insights. *Angew. Chem. Int. Ed.* **50**, 11062–11087 (2011).
19. R. Venkatasubramanian, R. T. Pickett, M. L. Timmons, Epitaxy of germanium using germane in the presence of tetramethylgermanium. *J. Appl. Phys.* **66**, 5662–5664 (1989).
20. R. Russotti, "Method of synthesis of gaseous germane," US 4,668,502 (1987).
21. C. Licht, L. T. Peiró, G. Villalba, Global substance flow analysis of gallium, germanium, and indium: Quantification of extraction, uses, and dissipative losses within their anthropogenic cycles. *J. Ind. Ecol.* **19**, 890–903 (2015).
22. J. Scoyer, H. Guislain, H. U. Wolf, Germanium and germanium compounds, in *Ullmann's Encyclopedia of Industrial Chemistry* (Wiley-VCH Verlag GmbH & Co. KGaA, 2000).
23. F. Melcher, P. Buchholz, Germanium, in *Critical Metals Handbook* (John Wiley & Sons, 2014), pp. 177–203.
24. M. L. Amadoruge, C. S. Weinert, Singly bonded catenated germanes: Eighty years of progress. *Chem. Rev.* **108**, 4253–4294 (2008).
25. A. A. El-Hadad, B. R. McGarvey, B. Merzougui, R. G. W. Sung, A. K. Trikha, D. G. Tuck, The reactions of elemental germanium with 3,5-di-*tert*-butyl-1,2-benzoquinone. *J. Chem. Soc. Dalton Trans.*, 1046–1052 (2001).
26. K. V. N. Esguerra, Y. Fall, L. Petitjean, J. P. Lumb, Controlling the catalytic aerobic oxidation of phenols. *J. Am. Chem. Soc.* **136**, 7662–7668 (2014).

27. S. L. James, C. J. Adams, C. Bolm, D. Braga, P. Collier, T. Friščić, F. Grepioni, K. D. M. Harris, G. Hyett, W. Jones, A. Krebs, J. Mack, L. Maini, A. G. Orpen, I. P. Parkin, W. C. Shearouse, J. W. Steed, D. C. Waddelli, Mechanochemistry: Opportunities for new and cleaner synthesis. *Chem. Soc. Rev.* **41**, 413–447 (2012).
28. T. Friščić, W. Jones, Recent advances in understanding the mechanism of cocrystal formation via grinding. *Cryst. Growth Des.* **9**, 1621–1637 (2009).
29. D. T. Tran, P. Y. Zavalij, S. R. J. Oliver, Tetrafluorodipyridinegermanium, $[GeF_4(C_5H_5N)_2]$. *Acta Crystallogr., Sect. E: Crystallogr. Commun.* **58**, m742–m743 (2002).
30. K. Hensen, A. Faber, M. Bolte, *trans*-Tetrabromobis(3,5-dimethylpyridine)germanium(IV), a non-merohedral twin. *Acta Crystallogr., Sect. C: Struct. Chem.* **55**, 1774–1775 (1999).
31. M. Bolte, K. Hensen, A. Faber, Complexes of germanium bromides with 4-picoline and 3,4-lutidine. *Acta Crystallogr., Sect. C: Struct. Chem.* **56**, e499–e500 (2000).
32. M. Bolte, K. Hensen, A. Faber, *trans*-Tetrachlorobis(4-methylpyridine)germanium(IV). *Acta Crystallogr., Sect. C: Struct. Chem.* **56**, e497–e498 (2000).
33. K. M. Baines, W. G. Stibbs, The molecular structure of organogermanium compounds. *Coord. Chem. Rev.* **145**, 157–200 (1995).
34. A. V. Lado, A. V. Piskunov, I. V. Zhdanovich, G. K. Fukin, E. V. Baranov, Novel germanium(IV) catecholate complexes. *Russ. J. Coord. Chem.* **34**, 251–255 (2008).
35. H.-C. Chiang, S.-F. Hwang, C.-H. Ueng, Bis(1,2-benzenediolato)dimethanolgermanium(IV). *Acta Crystallogr., Sect. C: Struct. Chem.* **52**, 31–33 (1996).
36. J. Zhao, L. Yang, J. A. McLeod, L. Liu, Reduced $GeO_2$ nanoparticles: Electronic structure of a nominal $GeO_x$ complex and its stability under $H_2$ annealing. *Sci. Rep.* **5**, 17779 (2015).
37. F. Qi, R. S. Stein, T. Friščić, Mimicking mineral neogenesis for the clean synthesis of metal–organic materials from mineral feedstocks: Coordination polymers, MOFs and metal oxide separation. *Green Chem.* **16**, 121–132 (2014).
38. M. Fishwick, M. G. H. Wallbridge, The properties of tetraallylsilane, -germane and -tin. *J. Organomet. Chem.* **25**, 69–79 (1970).
39. S. E. Allen, R. R. Walvoord, R. Padilla-Salinas, M. C. Kozlowski, Aerobic copper-catalyzed organic reactions. *Chem. Rev.* **113**, 6234–6458 (2013).
40. H. P. Withers, P. B. Henderson, "Process for purification of germane," US7087102-B2 (2006).
41. C. H. Yoder, T. M. Agee, A. K. Griffith, C. D. Shaeffer Jr., M. J. Carroll, A. S. DeToma, A. J. Fleisher, C. J. Gettel, A. L. Rheingold, Use of $^{73}$Ge NMR spectroscopy and x-ray crystallography for the study of electronic interactions in substitute tetrakis(phenyl)-, -(phenoxy)-, and (thiophenoxy)germanes. *Organometallics* **29**, 582–590 (2010).
42. The values obtained by Fishwick *et al.* are similar to our values: M. Fishwick, M. G. H. Wallbridge, *J. Organomet. Chem.* **25**, 69–79 (1970).


**Acknowledgments:** We would like to thank J. Zhao, National Synchrotron Radiation Research Center, Taiwan, and Shanghai Synchrotron Radiation Facility for technical support. **Funding:** Financial support for this project was provided by the Natural Sciences Engineering Research Council of Canada (418659-12, T.F. and K.M.B.), National Natural Science Foundation of China (21403147, 11404232, and U1432106), the Soochow University–Western University Center for Synchrotron Radiation Research, and the Collaborative Innovation Center of Suzhou Nano Science and Technology, Soochow University. **Author contributions:** J.-P.L., T.F., and K.M.B. conceived the experiments. M.G. synthesized and characterized the germanium bis-catecholates, M.K. synthesized and characterized the organogermanes. M.G. obtained the crystal structures, and, together with T.F., collected and interpreted the x-ray data. L.Y., J.A.M., and L.L. acquired and interpreted the XAS data. All authors contributed to manuscript preparation. **Competing interests:** All authors declare that they have no competing interests. **Data and materials availability:** All data needed to evaluate the conclusions in the paper are present in the paper and/or the Supplementary Materials. Additional data related to this paper may be requested from the authors. Crystallographic data for structures of **3**, **4**, and **5** are available free of charge from the Cambridge Crystallographic Data Centre (CCDC codes 1516976 to 1516978).

Submitted 13 January 2017
Accepted 7 March 2017
Published 5 May 2017
10.1126/sciadv.1700149

**Citation:** M. Glavinović, M. Krause, L. Yang, J. A. McLeod, L. Liu, K. M. Baines, T. Friščić, J.-P. Lumb, A chlorine-free protocol for processing germanium. *Sci. Adv.* **3**, e1700149 (2017).

# A chlorine-free protocol for processing germanium

Martin Glavinovic, Michael Krause, Linju Yang, John A. McLeod, Lijia Liu, Kim M. Baines, Tomislav Friscic and Jean-Philip Lumb

*Sci Adv* **3** (5), e1700149.
DOI: 10.1126/sciadv.1700149